# High-Frequency Characteristics of GaAlAs Injection Lasers

LUIS FIGUEROA, MEMBER, IEEE, CHARLES W. SLAYMAN, AND HUAN-WUN YEN

*Abstract*—This paper discusses the results of an extensive experimental study of the high-frequency characteristics of several commercial (GaAl)As injection lasers. The lasers tested included the Hitachi buried heterostructure (BH), the Hitachi channel substrate planar (CSP), the Mitsubishi transverse junction stripe (TJS), the General Optronics stripe (GO), and the RCA constricted double heterostructure (CDH). We find that the maximum practical analog modulation frequency $f_o$ is in the range of 5 GHz. This practical modulation frequency is limited by a combination of laser-relaxation resonance, laser parasitics, and drive current necessary for long-life operation. The relationship between laser-relaxation oscillation resonance frequency $f_o$ and drive current can be expressed as $f_o = K(I/I_{th} - 1)^{1/2}$ GHz where $I$ and $I_{th}$ are the laser drive and threshold currents, respectively. The value of $K$ is experimentally determined to lie in the range $3.0 < K < 5.3$ GHz for all the lasers studied. An equivalent circuit for the injection laser for frequencies in the range of 100 MHz–6 GHz has been experimentally determined. We find that the isolated injection laser can be modeled by the parallel combination of a resistance $R_j$ and a capacitance $C_j$. The product of $R_jC_j$ has been experimentally determined for both the Hitachi CSP and BH laser and lies in the range of $1\text{–}1.1 \times 10^{-10}$ s. The effect of laser mount and packaging can also be included in the equivalent circuit by the addition of series inductors and shunt capacitors.

Lastly, all injection lasers studied displayed a dip in the small signal modulation response prior to the onset of the relaxation oscillation resonance. In particular, there is a pronounced dip even for lasers with good lateral carrier confinement at dc, such as the buried heterostructure (BH). Previous workers have attributed the dip in the modulation response as resulting from either lateral diffusion of injected carriers, or the effect of junction capacitance. Our experimental results indicate that while the effect of the junction capacitance may play some role in explaining the dip for the BH laser, it is not the dominant mechanism. We speculate that lasers with good lateral carrier confinement at dc (BH) may suffer a significant degradation of carrier confinement at gigahertz rates. A simple qualitative model is proposed to explain this mechanism and methods for reducing the effect are discussed.

## I. INTRODUCTION

FUTURE microwave systems utilizing solid-state microwave devices, optical devices, and low-loss optical fibers offer the potential for improved performance and new capabilities in signal processing and communication systems. Such hybrid techniques can impact both analog and digital processing with the creation of delay lines, transversal filters, correlators, and adaptive array distribution networks operating in the popular microwave bands.

The key building block for these systems is a fiber-optic link (delay line) operating at microwave frequencies. A link consists of a microwave modulated light source, an optical fiber transmission line, and a high-speed optical detector. Significant advances in fiber-optics technology has led to the fabrication of fibers having bandwidths of tens of gigahertz, and just recently a 1 GHz analog fiber-optic link was demonstrated [1]. Recent experimental results [2], [3] on high-speed detectors indicate 3 dB bandwidths in excess of 8 GHz [2], [3]. The remaining concern is the high-frequency behavior of the injection laser.

In this paper we present an extensive study of the high-frequency (0.1–8 GHz) modulation and circuit characteristics of several existing commercial stripe geometry injection lasers. Our experimental results indicate that the maximum practical analog bandwidth is approximately 5 GHz. This limit results from the maximum bias that can be applied to the laser for reliable operation. Furthermore, our experimental results show that there is a significant drop in the modulation response of most injection lasers prior to the usual relaxation oscillation resonance. This dip is detrimental for analog systems since it will require the added complication of a gain equalization network in order to achieve uniform gain. We believe that the dip in the modulation response is produced by a combination of lateral carrier out-diffusion and the diffusion capacitance of the p–n junction. One of our significant results is that laser structures with good lateral carrier confinement at dc may suffer significant degradation of this property at GHz rates. An expression is given which shows the significance of this effect and methods for improving carrier confinement at GHz rates are discussed.

We have also been able to empirically determine an accurate circuit model for two widely used stripe geometry injection lasers (Hitachi CSP [1400], and the BH [2400]) from measurements of the diode impedance in the frequency range 0.1–6 GHz.

The paper is divided into four sections. In Section II we present the experimental arrangement. Section III describes the small signal modulation response of several commercial injection lasers, and simple theoretical models are used to explain the observed results. In Section IV, we summarize the experimental results and calculations, and discuss the degradation of lateral carrier confinement of gigahertz rates. Methods are discussed which can improve the frequency response of the injection lasers.

Manuscript received April 1, 1982; revised June 10, 1982.

L. Figueroa was with the Department of Electrical Engineering, North Carolina State University, Raleigh, NC 27650. He is now with the TRW Technology Research Center, El Segundo, CA 90245.

C. W. Slayman and H.-W. Yen are with Hughes Research Laboratories, Malibu, CA 90265.

0018-9480/82/1000-1706$00.75 

## II. High-Frequency Injection Laser Characteristics Experimental Arrangement

The experiments performed consist of the direct modulation and the $S$ parameter characterization of several commercially available injection lasers. The lasers used included the Hitachi BH [4] (buried heterostructure), BH/LOC [5] (BH/large optical cavity), Hitachi CSP [6] (channel substrate planar), Mitsubishi TJS [7] (transverse junction stripe), the General Optronics stripe [8] laser, and the RCA CDH [9] (constricted double heterostructure). Each laser used was mounted at the end of a microstrip fabricated from Au-plated alumina. The RF power was coupled via an APC-7 microstrip launcher. The optical signal was demodulated by a Rockwell GaAs/GaAlAs heterostructure photodiode [10]. A Hewlett-Packard network analyzer system HP-8410 (harmonic converter/$S$ parameter test set/phase magnitude display, and RF sweep generator) was used to characterize the frequency response of the laser-photodiode pair. Picosecond optical pulse measurements of the detector indicated a 3 dB bandwidth in excess of 6 GHz [11]. In Fig. 1 we show a block diagram of the frequency response experiment. The input RF power to the laser was less than -20 dBm for all cases considered. Fig. 2 shows the optics used to couple the laser radiation to the photodiode. A variable neutral density (ND) filter was used to prevent excess optical power from producing either nonlinear distortion or damaging the photodiode.

The $S$ parameters of several Hitachi lasers (CSP and BH) were measured by using an automatic network analyzer. A simple test fixture was designed and manufactured and consisted of a section of microstrip on an alumina substrate, an APC-7 launcher, a shorted reference line, and a copper block heat sink. The lasers were mounted at the end of the strip line opposite the launcher. From these measurements it was possible to derive a simple high-frequency equivalent circuit for the injection lasers.

Since the laser impedance is unmatched to the RF source, the actual RF power coupled into the laser is less than the -20 dBm produced by the RF source. However, the error produced by reflections is quite small, since the reflection coefficient of the laser/package for the BH and CSP type lasers is relatively independent of frequency for frequencies below 5-6 GHz. No measurements of the reflection coefficient were made for the other lasers tested.

## III. High-Frequency Modulation and $S$ Parameter Characterization of Injection Lasers

The frequency response of (GaAl)As injection lasers has been documented by many workers [12]-[15]. The earliest works are due to Ikegami and Suematsu [13], and Paoli and Ripper [14]. In the earlier works a simple rate equation approach was used to calculate the small signal modulation response of the injection laser. In more recent publications the effect of spontaneous emission [16], lateral carrier diffusion [17], gain saturation [18], multimode lasing [19], and laser geometry [20], have been considered. However, these models are not complete since they fail to include the effects of junction parasitics on the modulation response. In a recent paper Dumant *et al.* [21] has experimentally observed a dip

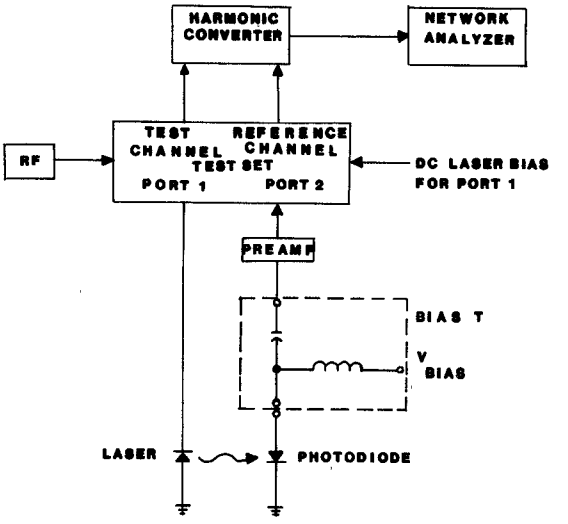


Fig. 1. Block diagram of the apparatus used for measuring small signal frequency response.

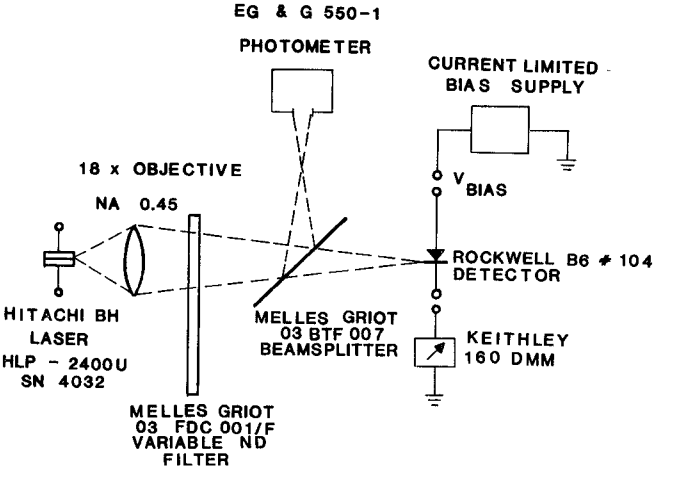


Fig. 2. Schematic of laser-photodiode optical arrangement.

in the modulation response of an injection laser prior to the relaxation oscillation resonance frequency. They have attributed this effect to the junction capacitance. However, the value for the junction capacitance is unrealistically large and the laser structure used was a simple stripe geometry laser where lateral out-diffusion effects are expected to play a significant role.

We have performed high frequency measurements on different laser structures with (BH) and without (CSP) lateral carrier confinement, and have observed a similar dip in the modulation response. The results reported here were first presented in [11]. The experimental results on the BH laser structure indicate that while junction diffusion capacitance plays some role in the observed dip in the modulation response, it is not the dominant mechanism. We believe that the dominant effect is enhanced lateral carrier out-diffusion which occurs at gigahertz rates. A model which gives an indication of this effect is described in Section IV.

The frequency response of an injection laser can be analyzed by using a pair of simple rate equations which describes the injected carrier and photon densities for a single longitudinal

mode [13]

$$\frac{dN_e}{dt} = \frac{J}{ed} - G(N_e - N_{om})S - \frac{N_e}{\zeta_s}$$

$$\frac{dS}{dt} = G(N_e - N_{om})S - \frac{S}{\zeta_p} + \beta N_e/\zeta_s \tag{1}$$

where $N_e$ is the electron inversion density, $S$ is the photon density, $J$ is the laser dc drive, $e$ is the electronic charge, $d$ is the thickness of the active region, $G(N_e - N_{om})$ is the laser gain (or loss), $N_{om}$ is the injected carrier density required for zero gain, $G$ is a constant related to the stimulated emission process, $\zeta_s$ is the spontaneous emission lifetime of the injected carriers, $\zeta_p$ is the photon lifetime, and $\beta$ is the spontaneous emission factor. This last factor gives us the fraction of the total spontaneous emission going into the lasing mode. The above equations neglect transverse optical confinement, current spreading, lateral out-diffusion of injected carriers, and junction parasitics. After our preliminary analysis we will comment on some of these effects and how they affect our results.

Since the equations in (1) are nonlinear, exact analytical solutions are difficult to obtain. However, approximations can be used to calculate the small signal modulation response of the injection laser. We simplify the equations by using the following normalization equations [13]:

$$t \equiv t/\zeta_s$$

$$n_e \equiv G\zeta_p N_e$$

$$n_{om} \equiv G\zeta_p N_{om}$$

$$s_p \equiv G\zeta_s S$$

$$j \equiv G\zeta_s\zeta_p \frac{J}{ed}$$

$$C \equiv (\zeta_s/\zeta_p).$$

Using the previous normalization procedure, the rate equation can be written as

$$\frac{dn_e}{dt} = j - s_p(n_e - n_{om}) - n_e$$

$$\frac{ds_p}{dt} = C[s_p(n_e - n_{om} - 1) + \beta n_e]. \tag{2}$$

To calculate the small signal ac response, we expand $j$, $n_e$, and $s_p$ into a dc and an ac portion, i.e.,

$$j = j_{(ac)} + j_{(dc)}$$

$$n_e = n_{e_{(dc)}} + n_{e_{(ac)}}$$

$$s_p = s_{p_{(dc)}} + s_{p_{(ac)}}. \tag{3}$$

Substituting (3) into (2) and neglecting second-order terms we can define a normalized modulation depth $F(\omega)$ as $(s_{p_{(ac)}}/j_{(ac)})$ and given by

$$F(\omega) = \frac{C(s_{p_{(dc)}} + \beta)}{(j\omega\zeta_s + s_{p_{(dc)}} + 1)\{j\omega\zeta_s - C(n_{e_{(dc)}} - n_{om} - 1)\} + C(s_{p_{(dc)}} + \beta)(n_{e_{(dc)}} - n_{om})}. \tag{4}$$

The value of $n_e$ can be found from the dc solution and is given by the solution to the quadratic equation

$$(1-\beta)\left(\frac{n_e}{n_{th}}\right)^2 - \left[\left(\frac{j}{j_{th}}\right) + (1-\beta) + \beta/jth\right]\left(\frac{n_e}{M_{e_{th}}}\right) + \frac{j}{j_{th}} = 0. \tag{5}$$

The normalized threshold current and photon density are:

$$j_{th} = n_{e_{th}} = 1 + n_{om}$$

$$s_{p(dc)} \cong \frac{(j-1)}{j_{th}} \cdot j_{th} \qquad j \geqslant j_{th}. \tag{6}$$

We can define a resonance frequency $f_{max}$ (relaxation-oscillation resonance) by finding the frequency for which the denominator of (4) is minimized. For $\beta = 0$, this occurs for

$$f_o = f_{max} = \frac{1}{2\pi}\left(\frac{1}{\zeta_s}\frac{1}{\zeta_p}\right)^{1/2}\left(\frac{j}{j_{th}} - 1\right)^{1/2}. \tag{7}$$

Thus, a plot of $f_{max}$ versus $(j/j_{th} - 1)^{1/2}$ gives a straight line with slope $1/2\pi(1/(\zeta_s\zeta_p))^{1/2}$. In our calculations we will assume that $\beta$ and $\zeta_p$ are empirical parameters which can be determined from the magnitude and frequency of the resonance in the small signal response. Although we use an empirical value for $\beta$, it is instructive to find the theoretical expression for $\beta$. Such an expression is helpful in qualitatively comparing lasers with different geometries and longitudinal mode structure. The spontaneous emission factor for a single longitudinal mode can be theoretically calculated from [16] as

$$\beta = \frac{\lambda^4}{2\pi n^3}\frac{1}{V}\frac{1}{\Delta\lambda}\Gamma \tag{8}$$

where $\lambda$ is the operating wavelength, $n$ is the index of refraction, $V$ is the volume of the injection laser, $\Delta\lambda$ is the bandwidth of the laser gain, and $\Gamma$ is the transverse optical confinement factor. This last factor, $\Gamma$, is the amount of optical energy in the active region relative to the total amount and can easily be calculated using the expressions derived by Botez [22]. The spontaneous emission factor $\beta$ is a damping term which tends to reduce the amplitude of the small signal resonance. Thus, from (8) we see that lasers with a small volume (i.e., a narrow stripe width) and a large number of longitudinal modes ($\beta_{eff} = N\beta$ where $N$ is the total number of longitudinal modes), will have a large $\beta$ and, hence, increased damping. We should further note that a finite $\beta$ has a negligible effect on the magnitude of the resonance frequency.

In Figs. 3-5 we show representative plots of the experimental small signal modulation response $|F(\omega)|_{exp}$ for several different commercially available stripe geometry lasers. The type of lasers used have been previously described in Section II. In all the experiments, at least two lasers of each type were used, and the results presented are typical of both lasers. Furthermore, all the lasers used display a normal noise frequency response and do not display any output instabilities [23]-[25]. The relaxation oscillation resonance can be observed in all the lasers tested. Furthermore, a dip in the modulation response prior to the relaxation oscillation resonance is observed in all the lasers tested. In Fig. 6 we show a representative plot of $f_{max}$ versus $(I/I_{th} - 1)^{1/2}$ for the CSP laser. All the lasers tested display a linear dependence for $f_{max}$ over

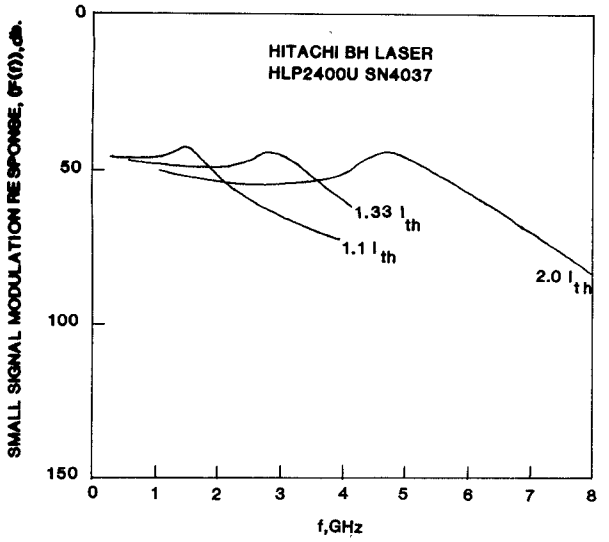


Fig. 3. Experimental small signal modulation response of the Hitachi BH laser.

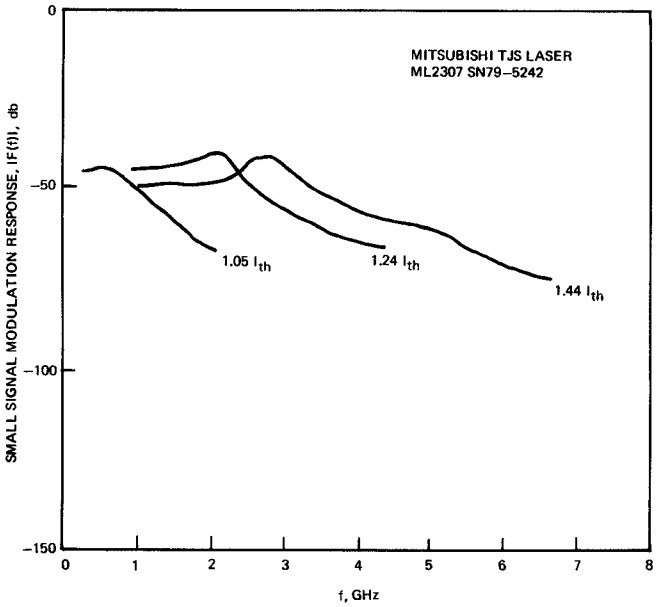


Fig. 4. Experimental small signal modulation response of the Mitsubishi TJS laser.

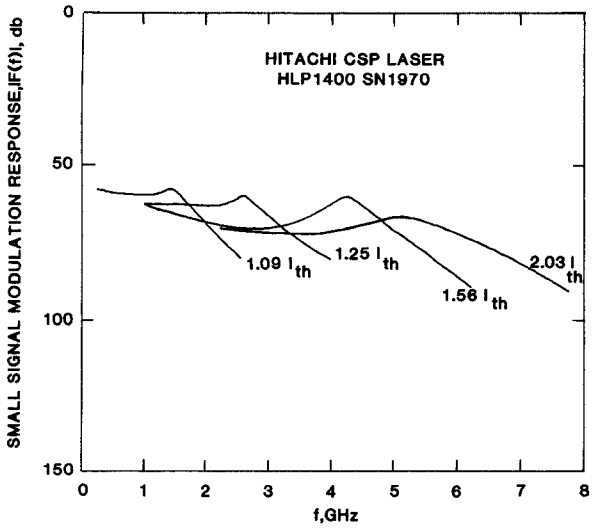


Fig. 5. Experimental small signal modulation response of the Hitachi CSP laser.

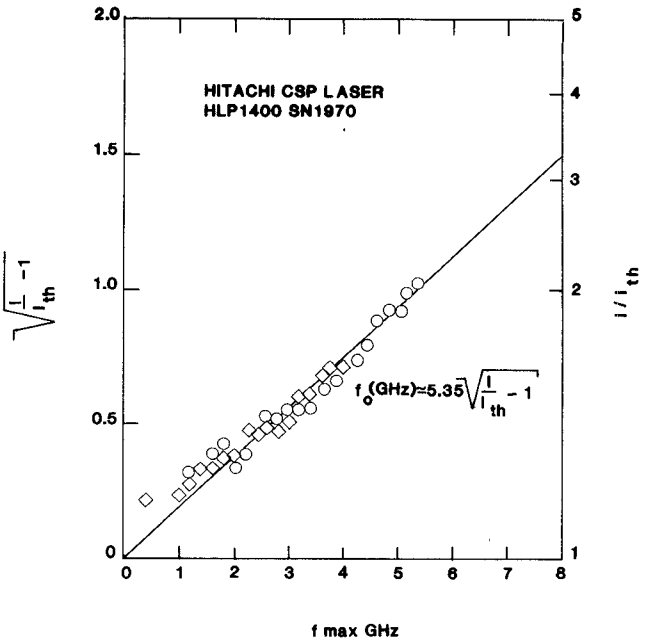


Fig. 6. Experimental relaxation oscillation resonance frequency $f_o$ as a function of dc bias for the Hitachi CSP.

the range of currents used in the experiments ($I < 2I_{th}$). Both the values of $1/2\pi\ (1/\zeta_s\zeta_p)^{1/2}$ and the peak magnitude of the resonance $\Delta R$ for all the lasers tested are tabulated in Table I. Several important results can be concluded. 1) The peak magnitude of the resonance is a function of the laser structure. Lasers having a smaller stripe width (BH, BH/LOC, and TJS) have a less pronounced resonance effect than lasers with a wider stripe width (CSP, G.O). 2) The dip in the modulation characteristics prior to the resonance is more pronounced in lasers without lateral carrier confinement (for example, CSP) compared to lasers having strong lateral carrier confinement (BH, TJS). However, we should emphasize that even for the BH laser there is a significant dip in the modulation response prior to the resonance. The TJS lasers show the least amount of dip of all the lasers tested. The value of $1/2\pi(1/\zeta_s\zeta_p)^{1/2}$ lies in the range of (3.7-5.3) GHz for all the lasers except the CDH structure. It appears that the resonance behavior of this laser is quite different from the other lasers tested. One possible reason for the behavior of the CDH laser is related to the laser mount and the relatively long wire connecting the laser and the mount. Such a mount will severely limit the frequency response of the laser [26].

In Figs. 7 and 8 we show the measured reflection coefficient $S_{11}$ (i.e., the input impedance of the laser) for the BH and CSP lasers, respectively. Each laser was characterized at several bias levels above threshold at frequencies ranging from 100 MHz to 10 GHz in 100 MHz steps. Each data point corresponds to a different input frequency. Starting from 100 MHz, the frequency increases clockwise and ends at 10 GHz. We did not observe any noticeable change in the laser reflection coefficient for currents above threshold. An attempt was made to derive an equivalent circuit for the injection laser (including bonding wire) based on the measured $S_{11}$ values. An appropriate equivalent circuit for frequencies in the range 0.1-6 GHz is shown in Fig. 9. The values of the circuit parameters are given in Table II and were derived using a computer program with a least-squares fit to the data in Figs. 7 and 8. The values ob-

TABLE I
EXPERIMENTAL VALUES OF $[1/(2\pi)][1/(\zeta_s\zeta_p)]^{1/2}$ AND RESONANCE AMPLITUDE $\Delta R$ FOR VARIOUS COMMERCIAL LASER STRUCTURES

| Laser Type | $(1/2\pi)(1/\zeta_s\zeta_p)^{1/2}$ (GHz) | Peak Magnitude of Resonance (a) dB $\Delta R$ |
|---|---|---|
| CSP | 5.3 | 4 |
| BH | 4.8 | 2 |
| BH/LOC | 3.7 | $\Delta<1$ |
| TJS | 4.2 | $\Delta<1$ |
| General Optronics | 4.5 | 12.8 |
| RCA/CDH(b) | 3.0 | 12 |

(a) Resonance amplitude is measured by finding the difference between the maximum and minimum small signal modulation response. The measurement is made for $(I/I_{th} < 1.1)$.

(b) Value is taken at $I=1.3I_{th}$. The shift in resonance frequency vs. current does not follow the expected result.

tained in Table I fit the data of Figs. 7 and 8 with an accuracy of 10-20 percent for frequencies in the range of 100 MHz-6 GHz. Calculated values are shown in Figs. 7 and 8 as solid points. In the circuit model, $R_J$ and $C_J$ are the diode diffusion resistance and capacitance, while $C_P$ and $L_S$ are the bonding wire capacitance and inductance. The latter two play a relatively insignificant role for frequencies less than 6 GHz.

In order to calculate the normalized small signal modulation response of the laser $|F(\omega)|$ we must take into account both the photon response (4) and the effect of the junction parasitics. The total normalized response $|F(\omega)|_n$ can be expressed as

$$|F(\omega)|_N = \frac{F(\omega)}{F(0)} \cdot \frac{H(\omega)}{H(0)} \tag{9}$$

where

$$H(\omega) = \frac{i_d}{V_{RF}} = \frac{1}{Z_T} \cdot \frac{1/j\omega C_p}{1/j\omega C_p + (j\omega L_s + Z_J)} \cdot \frac{1/j\omega C_J}{1/j\omega C_J + R_J} \tag{10a}$$

$$Z_T = R_g + Z_1; \quad \frac{1}{Z_1} = j\omega C_P + \frac{1}{(j\omega L_S + Z_J)}; \quad \frac{1}{Z_J} = j\omega C_J + \frac{1}{R_J} \tag{10b}$$

and $R_g$ is the source impedance. In all our calculations we will assume that the RF source impedance is 50 Ω. In Fig. 10 we show a representative plot of $|F(\omega)|_N$ for a laser having parameters appropriate for the BH. The parameters used are listed in Fig. 10. In particular the value of $\beta$ required to give approximate experimental agreement with respect to the magnitude of the resonance is $\beta = 10^{-2}$. This relatively large value of $\beta$ is not predicted by (8) which predicts values in the range of $10^{-4}$-$10^{-5}$. The discrepancy in the value of $\beta$ arises from neglecting the effects of lateral carrier out-diffusion in the simple rate equation model. The effect of lateral carrier out-diffusion is to produce an extra damping force on the injected carriers, which can be incorporated into the simple rate equations by just simply readjusting the value of $\beta$ empirically in order to fit the experimental data. However, we should note that this simple procedure does not explain the observation of a dip in the small signal frequency response. In order to predict the dip in the frequency response we must include both the effect of parasitics and lateral out-diffusion effects directly into our formulation. The value of $\zeta_s$ is taken to be nominally $3 \times 10^{-9}$ s. The value of $\zeta_p$ used in the calculation is obtained by comparing the calculated resonance frequency to the experimental value at $J/J_{th} = 1.50$. We should note, that this procedure is needed in order to get agreement between calculation and the experimental value. The value of $\zeta_p$ one obtains in this fashion is significantly less than the value obtained using the standard formula for photon lifetime which is given by

$$\zeta_p = \frac{n}{(\alpha + 1/l \ln 1/R)} c_o \tag{11}$$

where $\alpha(\sim 10\ \text{cm}^{-1})$ is distributed losses in the active region, $l$ is the laser cavity length (=300 μm), $R$ is the facet reflectivity (~0.3), and $c_o$ is the speed of light ($3 \times 10^{10}$ cm/s). Using (11) one obtains $\zeta_p \sim 2.8 \times 10^{-12}$ s, and in order to fit the calculation with experiment, one needs $\zeta_p = 1.17 \times 10^{-12}$ s. This rather large discrepancy can be explained [27] by assuming that the loss $\alpha$ in (11) is really the loss for $j = 0$ instead of $j = j_{th}$. This leads to a large loss, since for $j = 0$, the laser is unpumped and band-to-band absorption is large. Typical values for this loss are in the range of 100-200 $\text{cm}^{-1}$ [27]. Furthermore, the adjustment of the photon lifetime in the manner indicated by (11) and using the larger $\alpha$ implies that the laser resonance frequency is relatively insensitive to either mirror reflectivity or cavity length variations.

In Fig. 11 we plot the calculated and experimental magnitudes of the dip in the modulation response $\Delta_D$ versus current for the BH and CSP lasers.

The dip $\Delta_D$ is defined as the difference in magnitude between $F(f \to o)$ and $F(f_{min})$ where $f_{min}$ is the frequency where the magnitude drops to a minimum value. Note that there exists a significant discrepancy between the calculation and the experimental results. The calculated $\Delta_D$ is independent of the spontaneous emission factor $\beta$ for $\beta$ in the range of $10^{-2}$-$10^{-4}$.

## IV. DISCUSSION AND CONCLUDING REMARKS

In Section III we presented experimental and theoretical calculations on the small signal modulation response and $S$ parameter characterization for several commercially available GaAlAs/GaAs single-mode injection lasers. We believe the data provided will be useful to potential users of such lasers in high-frequency analog or digital fiber-optic links. The small signal resonance frequency $f_o$ sets an upper limit to the useful bandwidth for maximum analog modulation. The resonance frequency is found to vary as $K(I/I_{th} - 1)^{1/2}$ where $K$ ranges from 3.0 to 5.3 GHz in the lasers tested.

In all the lasers tested (except the TJS) we have observed a significant dip in the modulation response prior to the resonance. The dip has been explained by previous workers in terms of lateral carrier out-diffusion from the recombination

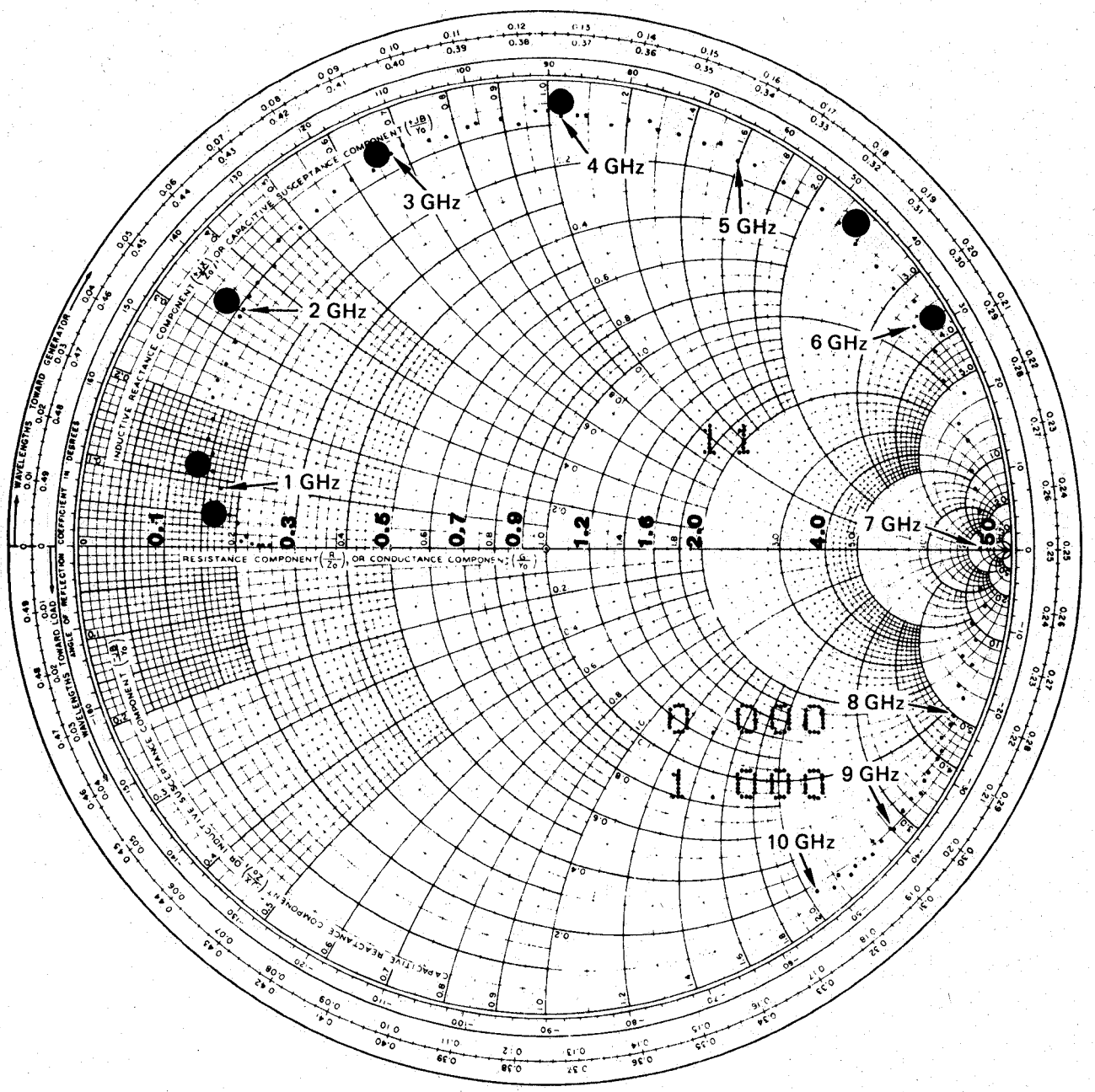


Fig. 7. Experimental measurements for the impedance of the Hitachi BH laser versus frequency for frequencies in the range of 100 MHz–10 GHz in 100 MHz steps. The Smith chart is normalized to 50 Ω. The drive current is $I = 1.2I_{th}$.

region. However, in lasers with good lateral carrier confinement, such as the BH laser, this mechanism did not appear to be valid. We have attempted to explain the observed small signal modulation response by including the junction diffusion capacitance in our model. The equivalent circuit was derived for the BH laser from the experimentally determined $S_{11}$. Using this equivalent circuit we can calculate the small signal modulation response. Although we calculate a small dip in the modulation response, there still exists a large discrepancy between the calculation and the experimental results. The measured values for $R_JC_J$ (i.e., diffusion resistance × diffusion capacitance) are in the range of $1 \times 10^{-10}$ s. However, a value of $R_JC_J \sim 3.2 \times 10^{-10}$ s is required to explain the experimental results. Such a large discrepancy cannot be accounted for by experimental error since it would imply an extremely large capacitance of ~32 pF for the BH laser, a value which is inconsistent with the results derived from the impedance measurements (see Table II). Our conclusion is that lateral out-diffusion of injected carriers must be significant in the BH laser at high frequencies.

In order to understand this effect we consider the lateral n-p heterojunction shown schematically in Fig. 12. Such a heterojunction is believed to be representative of a commercial BH laser [4], [5]. In order to have good lateral carrier confinement we require that the ratio of injected electrons $J_n$ from the n-side be much higher than the injected holes $J_p$ from the p-active region. We can get an order of magnitude estimate for $J_p/J_n$ at high frequencies by solving the carrier

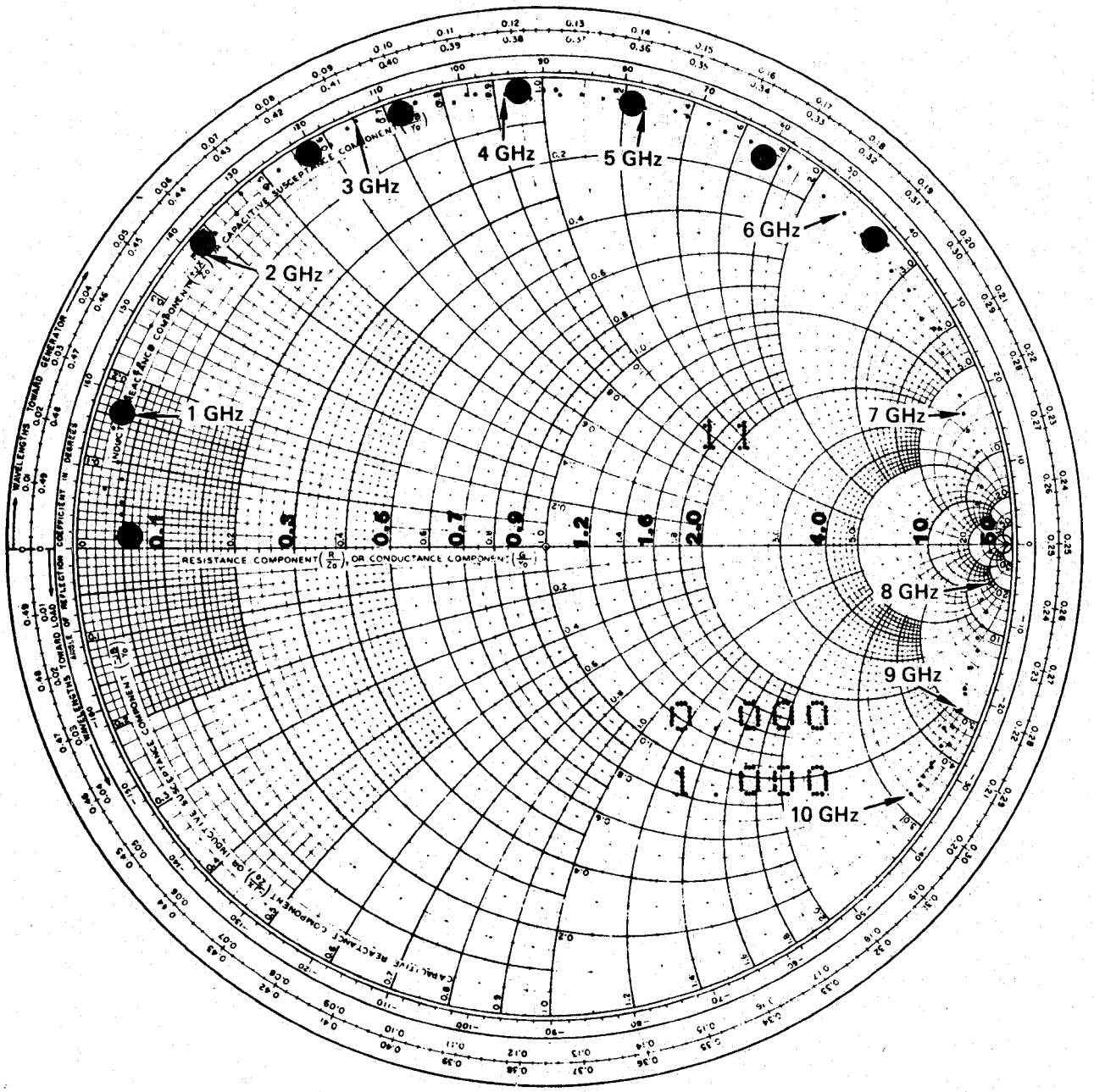


Fig. 8. Experimental measurements for the impedance of the Hitachi CSP laser versus frequency for frequencies in the range of 100 MHz–10 GHz in 100 MHz steps. The Smith chart is normalized to 50 Ω. The drive current is $1.2I_{th}$.

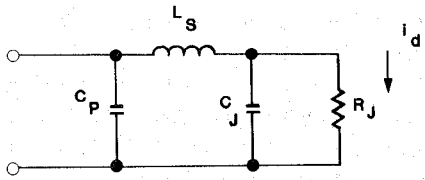


Fig. 9. Equivalent circuit for an injection laser for frequencies in the range of 100 MHz–6 GHz.

TABLE II
EQUIVALENT CIRCUIT PARAMETERS

| Laser Type | $C_P$, F | $L_G$, H | $C_J$, F | $R_J$, Ω |
|---|---|---|---|---|
| CSP | 0.315x10-12 | 1.318x10-9 | 40x10-12 | 2.75 |
| BH | 0.348x10-12 | 1.5x10-9 | 10x10-12 | 10 |

continuity equation with $e^{j\omega t}$ voltage and current variation in the quasi-neutral and p and n regions, small signal conditions, and assuming that the carrier recombination process in the p-active region is governed by a single lifetime (i.e., the stimulated lifetime). We would expect this lifetime to be a strong function of photon density and be much shorter than the spontaneous lifetime at currents sufficiently above threshold. For this case, and assuming that the lengths of the n- and p-active regions are much larger than a minority carrier diffusion length, we calculate that the $J_p/J_n$ ratio is given by [28]

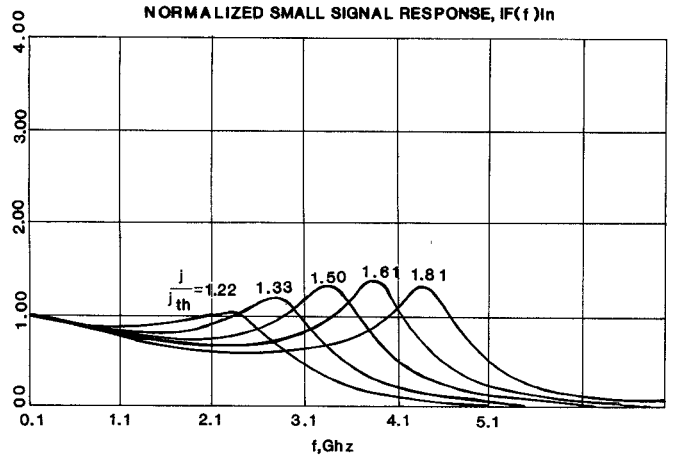


Fig. 10. Calculated normalized small signal modulation response $|F(f)|_n$ for an injection laser. The calculations include both the effect of spontaneous emission and parasitics. The parameters used are typical values for a BH laser, $\zeta_p = 1.17 \times 10^{-12}$ s, $\beta = 10^{-2}$, $\zeta_s = 3 \times 10^{-9}$ s. The parameters for the parasitics are obtained from Table II.

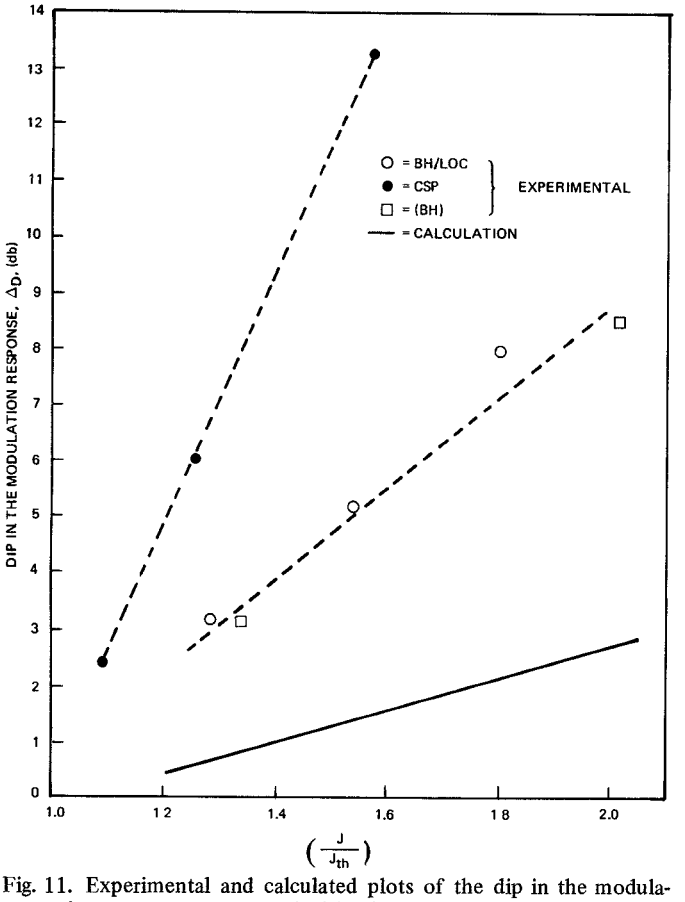


Fig. 11. Experimental and calculated plots of the dip in the modulation response $\Delta_D$ versus dc drive for several injection lasers.

$$D(\omega) = J_p/J_n \cong \frac{D_{pn}}{D_{np}} \frac{L_{pn}}{L_{np}} \frac{p}{n} \exp - \left(\frac{\Delta E_g}{KT}\right) \tag{12}$$

where $D_{pn}$, and $D_{np}$ are the minority carrier diffusion constants in the n and p regions, respectively, $p$ and $n$ are the effective background majority carrier densities in the p and n regions, respectively, $\Delta E_g$ is the difference in bandgaps between the

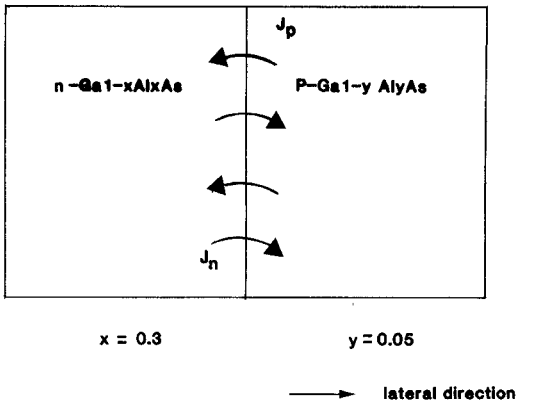


Fig. 12. Schematic of a lateral n($Ga_{1-x}Al_xAs$) – p($Ga_{1-y}Al_yAs$) heterojunction similar to that found in the BH laser structure. In the actual BH laser structure, there are two symmetric heterojunctions on each side of the active region.

n and p regions, $L_{np}$ and $L_{pn}$ are the frequency dependent diffusion lengths which are defined by

$$L_{np} = \frac{L'_{np}}{1 + j\omega\zeta_{np}} \tag{13a}$$

where $\omega$ is the radian frequency

$$L_{pn} = \frac{L'_{pn}}{1 + j\omega\zeta_{pn}} . \tag{13b}$$

In the previous equations $L'_{np}$ and $L'_{pn}$ are the diffusion lengths defined by

$$L'_{np} = \sqrt{(D_{np}\zeta_{np})}$$
$$L'_{pn} = \sqrt{(D_{pn}\zeta_{pn})} . \tag{14}$$

In order to evaluate (12) we use typical parameters for the BH laser [4], [5]. These values and the references used are summarized in Table III. We note in Table IV that although $J_p/J_n = D(\omega)$ is quite insignificant at dc ($\sim 1 \times 10^{-3}$), it can play a much larger role ($\sim 0.1$) for frequencies in excess of 1 GHz.

This result can help explain the small signal modulation response for the BH laser, since it implies that there is a significant amount of lateral carrier out-diffusion at gigahertz rates. The effect of lateral carrier out-diffusion on the small signal modulation response has been considered by Thompson [12] in great detail. Thompson considers the cases of lasers having no carrier confinement and lasers with ideal carrier confinement. The basic difference, in as far as modulation response is concerned, is the boundary conditions imposed on the carrier densities at the edges of the stripe region. For lasers having ideal carrier confinement, the boundary condition is $dn/dx = 0$ at the edge of the stripe region. Thus, no diffusion of carriers is possible at the edges of the stripe. For lasers having no carrier confinement the boundary condition is $n \to 0$ as $x \to \pm\infty$. Furthermore, Thompson concludes that lasers having no carrier confinement can experience large dips in the modulation response, while those lasers having ideal carrier confinement experience little or no dip. Thus,

TABLE III
PARAMETERS FOR CALCULATING REVERSE INJECTION RATIO $|J_p/J_n| = D$

| Parameter | Value |
|---|---|
| $D_{pn}(30)$ | 7.8 $cm^2/V\text{-}sec$ |
| $D_{np}(30)$ | 50 $cm^2/v\text{-}sec$ |
| n(5) | 1 x $10^{16}/cm^3$ |
| p*(31) | 2 x $10^{18}cm^3$ |
| $\zeta_{np}(32,33)$ | 100 x $10^{-12}s$ |
| $\zeta_{pn}(29)$ | 10 x $10^{-9}sec$ |
| $\Delta Eg(5)$ | 0.25 eV |
| $\frac{**}{KT}$ T=330°K | 0.0286 |

* This value is the carrier density required for lasing under nominal conditions.

** We have assumed the laser active p-region is at a temperature 30° higher than the n − (GaAl)As region.

TABLE IV
REVERSE INJECTION RATIO $|J_p/J_n| = |D|$ FOR BH LASER

| | |
|---|---|
| $D(f=0) = \left\|\frac{J_n}{J_p}\right\|$ | 1.24 x $10^{-3}$ |
| $D(f=1x10^9hz)$ | 0.063 |
| $D(f=2x10^9hz)$ | 0.082 |
| $D(f=3x10^9hz)$ | 0.089 |

there is a strong correlation between the dip in the modulation response and the degree of carrier confinement. From the calculated frequency dependence of $D(\omega)$, we can conclude that the carrier confinement properties of the BH laser degrade with frequency and it is therefore reasonable to expect a dip in the small signal modulation response. In order to properly include this effect in the rate equations we must modify the boundary conditions for the injected carriers at the edges of the stripe.

The important parameters in the determination of $D(\omega)$ are the doping density, minority carrier lifetime, and the bandgap of the n-$Ga_{1-x}Al_xAs$ layer. In our calculations we have assumed a minority carrier lifetime of $10 \times 10^{-9}$ s for the lightly doped n-type $Ga_{1-x}Al_xAs$ layer. This value is really appropriate for GaAs and not $Ga_{1-x}Al_xAs$ [29]. Furthermore, there is also an amount of uncertainty in the determination of $\Delta E_g$. This arises from the nonuniform temperature distribution of the laser and the possibility that the nonplanar expitaxial growth which is used in the fabrication of the BH laser may lead to a nonuniform Al distribution in the lateral direction. Thus we believe our value of $\Delta E_g$ is on the conservative side.

In order to improve the modulation response of the BH injection laser we can increase either the doping concentration or the Al concentration in the n-$G_{1-x}Al_xAs$ layer. Increasing the Al concentration by 5 percent at the heteroboundary should decrease the value of $D$ to ~0.01 for $f < 3$ GHz. We believe this value is sufficiently low to significantly reduce the dip in the modulation response. We should also note that (12) assumes that the width of the p-active region is longer than a carrier diffusion length. For $\zeta_{np} \sim 100 \times 10^{-12}$ s, the carrier diffusion length is ~0.7 $\mu$m. Thus, by reducing the mesa stripe width of the BH laser below 0.7 $\mu$m, we should be able to decrease $D(\omega)$. However, this method appears to present some practical difficulties with the present state-of-the-art photolithographic technology.

It is also worthwhile to point out that the mechanism described here can also explain the lack of a significant dip in the modulation response for the TJS laser. In the TJS laser, lateral carrier confinement is accomplished by a lateral $p^+$-n homojunction, where the confining layer is the $p^+$-layer (analogous to the n-$Ga_{1-x}Al_xAs$ layer in the BH) and the n-layer is the active region (analogous to the p-$Ga_{1-y}Al_yAs$ layer). Typically [7], the doping density in the $p^+$-side is a factor of 10 higher than the n-active layer. This has two advantageous effects. First, it decreases the doping concentration ratios in (12) and second, it decreases the lifetime of injected carriers in the confining layer. Both of these effects tend to reduce the reverse injection ratio $|J_n/J_p|$ and its frequency dependence. Thus, we expect little or no dip in the modulation response in agreement with experiment.

In summary we have presented experimental results on the high-frequency modulation and circuit characteristics of several 'commercial (GaAl)As injection lasers. Our results indicate that the maximum practical analog bandwidth for these lasers is less than 5 GHz. We have experimentally determined a useful laser equivalent circuit for the injection laser in the frequency range of 100 MHz–6 GHz. The intrinsic laser can be described in terms of a parallel combination of a junction resistance $R_J$ and junction capacitance $C_J$. Typical values for the product of $R_J \cdot C_J$ for the Hitachi CSP and BH lasers are $\sim 1 \times 10^{-10}$ s.

We have observed a dip in the small signal modulation response prior to the onset of the relaxation oscillation resonance in all of the injection lasers tested. Our experimental results appear to indicate that the dip is produced by lateral carrier diffusion even in lasers with good lateral carrier confinement such as the BH laser. A simple qualitative model has been presented which shows that the lateral confinement properties of the injection laser is a function of the RF frequency.

## ACKNOWLEDGMENT

The authors wish to thank K. Walsh of Hughes Fullerton for making laser impedance measurements. They also wish to thank E. Lin of Hughes Research Laboratories for the computer program used to find the equivalent circuit for the injection laser, Dr. D. Botez of RCA Research Laboratories for the CDH lasers provided, Dr. D. Law of TRW Research Center, and K. Nakano of the Rockwell Science Center for the APD used. This work was performed while one of the authors (L. Figueroa) was a member of the Technical Staff at Hughes Research Laboratories.

## REFERENCES


[1] C. W. Slayman and K. Lang, "Ghz bandwidth analog fiber optic system," Final Rep. under contract 4-x69-2908F-1.

[2] L. Figueroa and C. W. Slayman, "A novel heterostructure interdigital photodetector (HIP) with picosecond optical response," *IEEE Trans. Electron. Device Lett.*, vol. 2, p. 208, 1981.

[3] L. Figueroa, C. W. Slayman, and T. R. Ranganath, unpublished experimental results.

[4] T. Tsukada, "GaAs-$Ga_{1-x}Al_xAs$ buried-heterostructure injection lasers," *J. Appl. Phys.*, vol. 45, p. 4899, 1974.

[5] N. Chinone, K. Saito, R. Ito, K. Aiki, and N. Shige, "Highly efficient (GaAl)As buried-heterostructure lasers with buried optical guide," *Appl. Phys. Lett.*, vol. 35, p. 513, 1979.

[6] K. Aiki, M. Nakamura, T. Kuroda, J. Umeda, R. Ito, N. Chinone, and M. Maeda, "Transverse mode stabilized $Al_xGa_{1-x}As$ injection lasers with channeled-substrate-planar structures," *IEEE J. Quantum Electron.*, vol. QE-14, p. 89, 1978.

[7] H. Namazaki, H. Kan, M. Ishii, and A. Ito, "Transverse-junction stripe geometry double-heterostructure lasers with very low threshold current," *J. Appl. Phys.*, vol. 45, p. 2785, 1974.

[8] General Optronics Company, S. Plainfield, NJ 07080.

[9] D. Botez and P. Zory, "Constricted double-heterostructure (AlGa)As diode lasers," *Appl. Phys. Lett.*, vol. 32, p. 261, 1978.

[10] D. Law, K. Nakano, and L. R. Tomasetta, "III-V Alloy heterostructure high speed avalanche photodiodes," *IEEE J. Quantum Electron.*, vol. QE-15, p. 549, 1979.

[11] L. Figueroa, C. W. Slayman, and H. W. Yen, "Optical-microwave interactions in semiconductor devices," Final Rep. under DARPA contract N00173-78-C-0192, Mar. 1981.

[12] See, for review G.H.B. Thompson, *Physics of Semiconductor Laser Devices.* New York: Wiley, 1980, ch. 7.

[13] H. Kressel and J. K. Butler, *Semiconductor Lasers and Heterojunction LED's.* New York: Academic, 1977, p. 562.

[14] T. Ikegami and Y. Suematsu, "Resonance-like characteristics of the direct modulation of a junction laser," *Proc. IEEE*, vol. 55, p. 122, 1967.

[15] T. L. Paoli and J. E. Ripper, "Direct modulation of semiconductor lasers," *Proc. IEEE*, vol. 58, p. 1457, 1970.

[16] Y. Suematsu, S. Akiba, and T. Hong, "Measurement of spontaneous-emission factor of AlGaAs double-heterostructure semiconductor lasers," *IEEE J. Quantum Electron.*, vol. QE-13, p. 596, 1977.

[17] M. Ito, T. Ito, and T. Kimura, "Measurement of spontaneous-emission factor of AlGaAs double-heterostructure semiconductor lasers," *IEEE J. Quantum Electron.*, vol. QE-15, p. 6168, 1979.

[18] D. J. Chanin, "Measurement of spontaneous-emission factor of AlGaAs double-heterostructure semiconductor lasers," *J. Appl. Phys.*, vol. 50, p. 3858, 1979.

[19] K. Petermann, "Calculated spontaneous emission factor for double heterostructure injection lasers with gain-induced waveguiding," *IEEE J. Quantum Electron.*, vol. QE-15, p. 566, 1979.

[20] E. Bourkoff, D. Kerps, and R.W.H. Englemann, "Modulation characteristics of semiconductor laser devices," *IEEE Trans. Electron Devices*, vol. ED-27, p. 2180, 1980.

[21] J. M. Dumant, Y. Guillausseau, and M. Monerie, *Opt. Commun.*, vol. 33, p. 188, 1980.

[22] D. Botez and M. Ettenberg, "Beam width approximations for the fundamental mode in symmetric double-heterojunction lasers," *IEEE J. Quantum Electron.*, vol. QE-14, p. 827, 1978.

[23] B. W. Hakki, "Instabilities in output of injection lasers," *J. Appl. Phys.*, vol. 50, p. 5360, 1979.

[24] ——, "Optical and microwave instabilities in injection lasers," *J. Appl. Phys.*, vol. 51, p. 68, 1980.

[25] L. Figueroa, "Study of mode-locking in (GaAl)As injection lasers," *IEEE J. Quantum Electron.*, vol. QE-17, pp. 1074–1085, June 1981.

[26] D. Botez, private communication.

[27] T. L. Paoli, "Magnitude of the intrinsic resonant frequency in a semiconductor laser," *Appl. Phys. Lett.*, vol. 39, p. 522, 1981.

[28] A. G. Milnes and D. L. Feucht, *Heterojunction and Metal-Semiconductor Junctions*, 1972, p. 15.

[29] H. Kressel and J. K. Butler, *Semiconductor Lasers and Heterojunction LED's.* New York: Academic, 1977, p. 260.

[30] S. Sze, *Physics of Semiconductor Devices.* New York: Wiley, 1980, ch. 1.

[31] H. Kressel and J. K. Butler, *Semiconductor Lasers and Heterojunction LED's.* New York: Academic, 1977, p. 263.

[32] ——, *Semiconductor Lasers and Heterojunction LED's.* New York: Academic, 1977, p. 558.

[33] B. Zee, "Broadening mechanisms in semiconductor (GaAs) lasers: Limitations to single mode emission," Ph.D. dissertation, Univ. of California, Berkeley, CA, 1977, ch. 3.


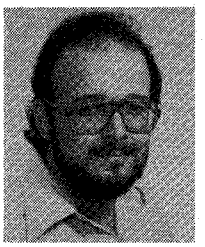

**Luis Figueroa** (S'78–M'78) received the B.S., M.S., and Ph.D. degrees in electrical engineering from the University of California, Berkeley, in 1973, 1976, and 1978, respectively. His Ph.D. thesis work was concerned with the fabrication, characterization, and analysis of GaAs semiconductor lasers with lateral mode control.

From September 1978 to July 1981 he was a member of the technical staff at Hughes Research Laboratories, Malibu, CA, where he worked on optical–microwave interactions in III–V semiconductors. His research has included fabrication and characterization of GaAs MESFET's for high-speed optical detection, high-frequency characterization of injection lasers, short pulse generation and mode-locking of injection lasers, fabrication and characterization of high-speed optical detectors, and fiber-optic sensors. In August 1981 he joined the Department of Electrical Engineering, North Carolina State University, Raleigh. Presently, he is with the TRW Technology Research Center, El Segundo, CA.

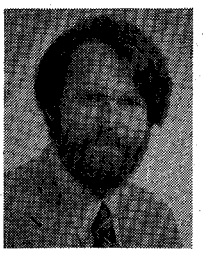

**Charles W. Slayman** was born in Detroit, MI, on April 19, 1952. He received the B.A. degree in physics in 1974 and the Ph.D. degree in electrical engineering and computer science in 1980, both from the University of California, Berkeley. His doctoral work consisted of fabrication and characterization of metal-oxide–metal junctions for use as UV photodetectors and millimeter wave (36 and 72 GHz) mixers and detectors.

In 1979 he joined Hughes Research Laboratories, Malibu, CA, where he has worked on optical-microwave devices, high-frequency semiconductor laser modulation, optical effects in microwave devices, high-speed photodetectors, and microwave bandwidth fiber optic links. He is currently engaged in masked ion beam lithography and characterization of electron beam lithography for submillimeter device fabrication.

**Huan-wun Yen** was born in Taipei, Taiwan, on January 24, 1948. He received the B.S. degree from National Taiwan University, Taiwan, and the M.S. and Ph.D. degrees from the California Institute of Technology, Pasadena, all in electrical engineering, in 1970, 1972, and 1976, respectively. His thesis work was on the development of GaAs distributed feedback and Bragg reflector lasers.

Since 1976 he has been with the Hughes Research Laboratories, Malibu, CA. He is presently Head of the Guided Wave Applications Section, Optical Circuits Department. His research interests include optoelectronic components, integrated optics, fiber optics, and optical-microwave interactions.

Dr. Yen is a member of the Optical Society of America.